Heterocyclic Letters
Vol. 14| No.2|407-422|Feb-April|2024
ISSN : (print) 2231–3087 / (online) 2230-9632
CODEN: HLEEAI
http://heteroletters.org

BIOLOGICALLY POTENT NOVEL HETEROCYCLIC AZOMETHINES AND THEIR CO (II) METAL COMPLEXES: GREEN SYNTHESIS, CHARACTERIZATION AND MOLECULAR DOCKING STUDIES WITH SARS-COV-2 MAIN PROTEASE 6LU7

Arghya De[a], Ritu Tomar[a*]

[a]*Department of Chemistry, Bhupal Noble's University, Udaipur-313001, India*
E-mail: ritutomarbnu@gmail.com

Abstract
Over the last few years, the pharmaceutical and chemical industries have been on the lookout for new technologies that will make large-scale synthesis easier, faster and cost effective. Chemical synthesis mediated by microwave irradiation (MW) is one of the most promising methods because it has several advantages, including higher atom economy, environmental friendliness, a straightforward work-up procedure, and a good-to-high yield in relatively mild conditions. Keeping all these facts under consideration during the present investigations synthesize some new Cobalt (II) Schiff base complexes using microwave irradiation technique as well as conventional heating. This paper focused to describe the green synthesis, characterization, biological studies and molecular docking evaluation of novel heterocyclic Schiff base ligands and their cobalt (II) complexes. Azomethine ligands namely (E)-2-((4-methylthiophen-2-yl)methylene)hydrazine-1-carboxamide(IL-1), (E)-2-((4-methylthiophen-2-yl)methylene)hydrazine-1-carbothioamide (IL-2), Ethyl (E)-2-((4-methylthiophen-2-yl)methylene)hydrazine-1-carboxylate(IL-3), O-ethyl (E)-2-((4-methylthiophen-2-yl)methylene)hydrazine-1-carbothioate (IL-4) are synthesized using cellulose sulfuric acid as a catalyst. Further the molecular structure of these compounds were established using ^{1}H-NMR, ^{13}C-NMR, LCMS, UV-Vis, and FTIR spectroscopic data, elemental analysis, molar conductivity measurements, X-ray powder diffraction and Thermo Gravimetric analysis. The ability of the ligands and complexes to suppress the growth of a number of fungal and bacterial strains has been tested. The SARS-CoV-2 enzyme 6LU7 was used to perform a molecular docking investigation on Schiff bases and their metal conjugates. These investigations shed light on the potential for Schiff base derivatives to bind to SARS-CoV-2 proteins, which could lead to the development of a more effective treatment.

Keywords: Cobalt (II) complexes; Heterocyclic N, O and S donor Schiff base ligands; Cellulose Sulfuric Acid(CSA);Spectral studies; Molecular docking COVID-19; Antimicrobial activity.

Introduction

The novel coronavirus (2019-nCoV) has recently been discovered in Hubei Province, P.R. China. On January 10, 2020, the whole-genome chain of 2019-nCoV was disclosed for the

first time. This attribute of transmission prompts the likelihood of transmission from animals to humans. The 2019-nCoV, also known as SARS-CoV-2 (strict acute respiratory syndrome coronavirus), is highly contagious and can cause mild to severe respiratory tract infections. The scope of 2019-nCoV has attracted a lot of attention for researchers.[i-iv] The increasing environmental consciousness throughout the world has put a pressing need to develop an alternate synthetic approach for biologically and synthetically important compounds. This requires a new approach, which will reduce the material and energy intensity of chemical processes and products, minimize or eliminate the dispersion of harmful chemicals in the environment in a way that enhances the industrially benign approach and meets the challenges of green chemistry. Green chemistry is defined as the utilization of a set of principles that reduces or eliminates the use or generation of hazardous substances in the design, manufacture and application of chemical products. The use of microwave ovens in chemical synthesis and analysis has increasingly grown in importance, due to its ability to dramatically reduce reaction times, improve yield, and simplify procedures. [v]In recent years, science and technology have shifted their focus to more environmentally conscious natural product resources and recyclable catalysts. As a result, natural biopolymers are appealing components for solid support catalysts.[vi-vii]For acid catalyzed reactions, cellulose sulfuric acid (CSA) has emerged as a viable biopolymeric reusable solid support acid catalyst. [viii]The azomethine N-atom, as well as other donor atoms like the O, S atoms, play an important role in coordination chemistry by easily coordinating with metal atoms to form different complexes. [ix-xi]Recently, significant progress has been made in the production and identification of complexes, especially Schiff bases, for use as catalysts. [xi]The science of semi/thiosemicarbazones and Schiff bases of thioethyl/ethylcarbazate have gotten impressive consideration taking into account their variable holding modes, promising biological ramifications, ion-sensing power and structural diversity. [xii-xv] Metal buildings, specifically of progress metal particles, are significant in numerous spaces of science, including catalysis, medication (analysis and treatment), plan of high worth materials, logical science and as model mixtures with the design and capacity of metalloproteins.[xvi-xvii]Cobalt (II) is an interesting d-block transition metal, which has been set up to be organically significant at all the degrees of living beings.[xviii] Between of two stable oxidation state of cobalt, cobalt (II) has been displayed to assume a positive part in controlling sugar and lipid digestion. The biological activity of Schiff base metal complexes is one of the most important areas of research, with the main goal being the identification of safe and effective therapeutic agents for the treatment of bacterial infections and malignancies. A wide range of pharmacological actions can be found in Schiff base metal complexes. Transition metal complexes with Schiff base ligands carrying "N", “S” and "O" donor atoms, for example, are particularly interesting because of their biological capabilities, which include antibacterial, antifungal, anti-inflammatory, antioxidant, antitubercular, analgesic, and anthelmintic activities.[xix-xxiii]

To the best of our knowledge the use of CSA as an organocatalyst for the synthesis of Schiff bases has not been reported previously. In light of the aforementioned wide-ranging applications, in the present work, we discussed the roles of green catalyst cellulose sulfuric acid (CSA) during the synthesis of novel heterocyclic Schiff base derivatives (IL-1, IL-2, IL-3, and IL-4) derived from condensation of aldehyde with desired amines and their novel octahedral Cobalt (II) complexes in microwave irradiation as well as conventional techniques. We discussed the synthesis path, structural geometry and kinetic parameters of the Schiff bases and their complexes utilizing NMR (^{1}H, ^{13}C), FT-IR, electronic spectroscopy, LCMS, PXRD, elemental analysis, thermo gravimetric analysis (TGA) etc. Finally, the complexes were computationally docked to SARS-CoV-2 protein after spectroscopic characterization to determine their capability to bind with the target

enzyme/receptor. *In vitro* (antibacterial) and *in vitro* (antifungal) experiments on the newly synthesized Schiff base ligands and their complexes were done concurrently to investigate the possibility of interactions with fungi and bacteria.

Experimental

Materials and methods

Used chemicals and solvents were analytical grade and utilized exactly as received from vendor. The molecular weights were determined by the Rast Camphor method.[xxiv] The metal contents were analyzed gravimetrically. A Carlo-Erba 1108 analyzer was used to perform the elemental studies (C, H, N, S) and 10^{-3} M DMF solutions were used to measure conductivity with a Lab India/PICO+ instrument. Melting points were determined with a Büchi Melting point M-565 detector. Powder XRD was performed on the fifth generation Rigaku (Model no Mini Flex 600) instrument. Using a Bruker V-22 spectrophotometer and a KBr disc, infrared spectra in the range 4000–400 cm^{-1} were recorded. Using DMSO-d_6 as a solvent, NMR spectra (^1H and ^{13}C) were obtained on a JEOL ECS-400 MHz machine. On METTLER-TOLEDO instrument thermo gravimetric analyses were performed at temperature range 50-800°C. Waters/H-class plus QDA was used to predict LC-MS. HPLC analyses were performed on Agilent/1260 Infinity-II. A Shimadzu/UV-2450 spectrophotometer was used to conduct UV-vis tests in 10^{-3}M DMSO solutions. Molecular docking studies were performed by AutoDock Vina (CB-Dock –Yang Cao Lab) software.

Synthesis

Preparation of green catalyst: cellulose sulfuric acid (CSA)

Cellulose sulfuric acid was produced and characterized using well-established methods (Scheme-1).[xxv] To 100 ml 4-necks RBF took 5 gm cellulose in 200 ml dried chloroform at 20-30°C. Cooled the reaction mixture to 0-2°C and slowly dropwise added 1 gm of chlorosulfonic acid (9 mmol) to the mixture during 1.5-2.0 hrs. During chlorosulfonic acid addition white fumes of HCl gas was observed. After complete addition of chlorosulfonic acid, allowed the reaction mass to come at room temperature and stirred the reaction mixture for 2.0 hrs at 20-30°C. Then filtered the mixture under reduced pressure and washed with 30 ml of chloroform at 20-30°C. 5.22 gm suck dried cellulose sulfuric acid solid was isolated. The sulphur concentration of the samples was 0.54 mmol g^{-1} for cellulose sulfuric acid, as measured by traditional elemental analysis. By acid–base titration, the number of H^+ sites on the cellulose–SO_3H was 0.51 mmol g^{-1}, which was extremely near to the sulphur concentration. The majority of the sulphur species on the sample were in the form of sulfonic acid groups, according to these findings.

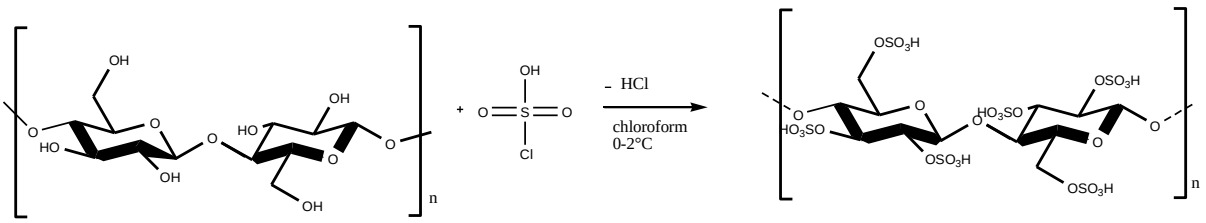

Scheme-1: Showing synthesis and structure of cellulose sulfuric acid

General procedure for the synthesis of novel Schiff base ligands (IL-1, IL-2, IL-3 and IL-4)

Two different routes were used for the synthesis of (IL-1, IL-2, IL-3 and IL-4) ligands.

(A) Microwave method: In microwave assisted synthesis of the ligands, (E)-1-((4-methylthiophen-2-yl)methylene)semicarbazide (IL-1), (E)-1-((4-methylthiophen-2-yl)methylene)thiosemicarbazide (IL-2), Ethyl (E)-2-((4-methylthiophen-2-yl)methylene)hydrazine-1-carboxylate (IL-3) and O-ethyl (E)-2-((4-methylthiophen-2-

yl)methylene)hydrazine-1-carbothioate (IL-4) were synthesized by the condensation of an equimolar mixture of 4-methylthiophene-2-carbaldehyde (11.15 mmol) with semicarbazide hydrochloride (11.15 mmol) (in the presence of sodium acetate), thiosemicarbazide (11.15 mmol), ethyl carbazate (11.15 mmol) and ethyl thiocarbazate (11.15 mmol)in 1:1 molar ratio using a conventional microwave oven in the presence of a ethanolic solution (5 ml) of cellulose sulfuric acid (0.1 g), respectively. The reactions were completed in a short period of 3.0-4.5 min. Solid white suspension was filtered, washed with chilled ethanol at 0-5°C and dried at 40°C under vacuum oven over P_4O_{10} for 5-6 hr. HPLC was used to monitor the progress of reaction and purity of desired solid. These ligands were also synthesized by above Microwave method without using CSA catalyst which took more times, 6-8 mins instead of 3.0-4.5 min.

(B) Thermal method: For comparison purpose, the above ligands were also synthesized by a thermal where instead of few drops of alcohol, the hot ethanolic solution (20 ml) of 4-methylthiophene-2-carbaldehyde (11.15 mmol) was mixed with hot ethanolic solution (20 ml) of semicarbazide hydrochloride (11.15 mmol) (in the presence of sodium acetate), thiosemicarbazide (11.15 mmol), ethyl carbazate (11.15 mmol) and ethyl thiocarbazate (11.15 mmol in 1:1 molar ratio using cellulose sulfuric acid (0.1 g) as a catalyst, respectively. The contents were refluxed for about 3.0–4.0 hrs on a water bath. Solid white suspension was filtered, washed with chilled ethanol at 0-5°C and dried at 40°C under vacuum oven over P_4O_{10} for 5-6 hr. HPLC was used to monitor the progress of reaction and purity of desired solid. These ligands were also synthesized by above Thermal method without using CSA catalyst which took more times, 6-7 hrs instead of 3.0-4.0 hrs. A schematic illustration of the synthesis of Schiff base ligands is depicted in **Scheme-2.**

General procedure for the synthesis of novel Cobalt (II) metal complexes:

For the comparison purpose, two different routes were considered for the synthesis of the Co(II) metal complexes with all respective ligands, (IL-1, IL-2, IL-3 and IL-4).

(A) Microwave method: In microwave assisted synthesis, the complexes were prepared by irradiating the 8 ml dry ethanolic reaction mixture of $Co(OAc)_2.4H_2O$ and the respective ligands (IL-1, IL-2 , IL-3 and IL-4) in 1:1 and 1:2 molar ratios using NaOH in appropriate stoichiometric proportions. The mixture was stirred continuously using domestic microwave for 5-8 mins. The resulting mixture was concentrated under reduced pressure. The distinct coloured precipitates were separated and washed with hexane as well as water multiple times to remove sodium acetate formed during the course of the reaction. Then desire products were recrystallized with chloroform and let to dry.

(B) Thermal method: These complexes were also synthesized by the thermal method where instead of 5–8 min, reactions were completed in 11–13 hrs and the yield of the products was also less than that obtained by the microwave assisted synthesis. In this method the ethanolic solution of $Co(OAc)_2.4H_2O$ (25 ml) was added to the ethanolic solution (25 ml) of ligands (IL-1, IL-2 , IL-3 and IL-4) in 1:1 and 1:2 molar ratios using NaOH in appropriate stoichiometric proportions. The resulting mixture was heated under reflux for 11-13 hrs. The resulting mixture was concentrated under reduced pressure. The distinct coloured precipitates were separated and washed with hexane as well as water multiple times to remove sodium acetate formed during the course of the reaction. Then desire products were recrystallized with chloroform and let to dry. A comparison between thermal method and MW method is given in **Table-1 (See Supporting Information).**

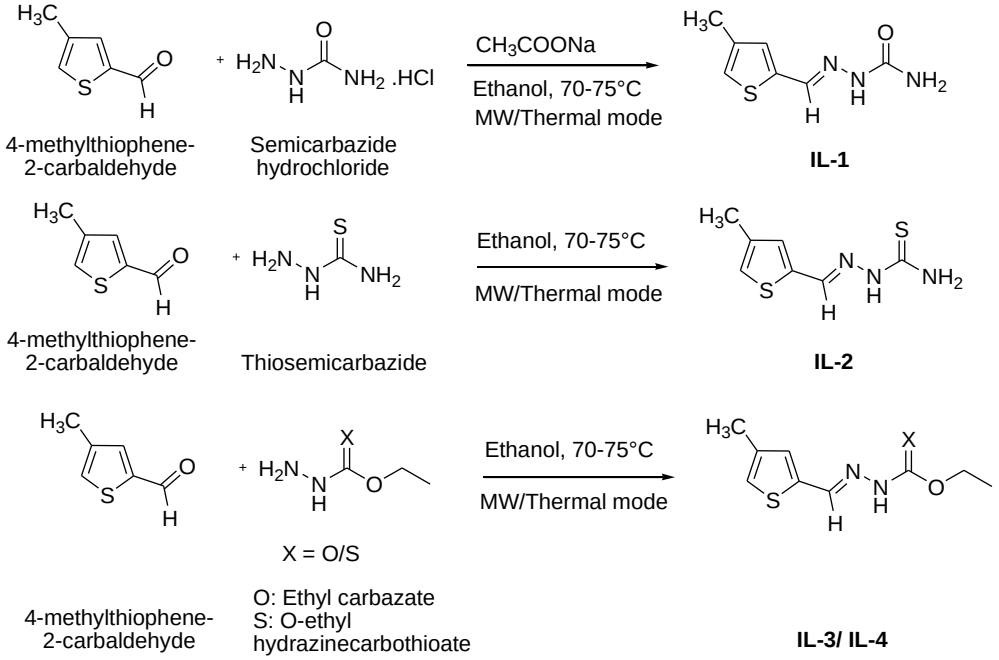

Scheme-2: Showing synthesis and structure of novel Schiff base ligands

Biological Studies

Antifungal activity

The antifungal screening of the novel Schiff base ligands and their Cobalt (II) metal complexes was tested by agar plate procedure[xxvi, xxvii] against the two pathogenic fungi *C. albicans* and *A. Niger* utilizing the potato dextrose agar medium having the composition: glucose 20 g, starch 20 g, agar-agar 20 g and distilled water 1000 ml. Methanol solutions of the test compounds at fixed concentration of 50, 100, 200 ppm were prepared and afterward were blended in with the medium. The medium then, at that point was filled into Petri plates and the spores of organisms were set on the medium with the assistance if inoculum's needle. These Petri plates were enclosed by the polythene containing a couple of drops of methanol and were put in an incubator at 25 ± 2 °C. After 96 hours of incubation at room temperature (25°C), the antifungal activity was measured. Controls were performed, with three replicates in each case. After 4 days, the fungal colony was estimated using the following formula:

% inhibition = $\frac{(c-T)}{C}$ x 100

Where, the diameters of the fungus colonies in the control and test plates, respectively, are C and T.

Antibacterial activity

For the primary selection of compounds as therapeutic agents, disc diffusion method[xxvii, xxviii] is commonly used *in-vitro* antibacterial screening. The method is primarily a qualitative or semi-quantitative test that indicates microorganism susceptibility or resistance to test materials, as well as a compound's bacteriostatic or bactericidal activity. Gram-positive (*B. subtilis*) and Gram-negative (*E. coli*) bacteria were used to test the antibacterial activity of the ligands and their cobalt complexes. The peptone 5 g, beef extract 5 g, NaCl 5 g, agar-agar 20 g, and distilled water 1000 ml of the nutritional agar medium was pipetted out into the Petri plates. 5 ml of warm seeded agar was added after solidification. The seeded agar was made by cooling the molten agar to 40°C and then added 10 ml of bacterial solution. The compounds were dissolved in methanol at concentrations of 500 and 1000 ppm. Whatman No. 1 filter paper discs with a diameter of 5 mm were soaked in these solutions at various concentrations. The discs were dried and placed at a proper distance on the medium that had

previously been seeded with organisms on Petri plates. The Petri plates were kept in an incubator for 24 hours at 28±2 °C. The sizes of the compounds inhibitory zones were compared to those of a conventional antibiotic (Streptomycin). The inhibitory zone that formed surrounding each disc containing the test chemicals was measured precisely in millimeters.

Determination of minimum inhibitory concentration (MIC):

The lowest concentration of test agent that prevented observable growth of bacteria after 22 hours of incubation at 37°C is known as the Minimum Inhibitory Concentration, or MIC. The MIC is calculated using a semi-quantitative test process that approximates the lowest concentration of antimicrobial required to suppress bacteria growth. The liquid dilution method[xxix] was used to determine the lowest inhibitory concentration. With aqueous methanol solvent, stock solutions of selected ligands (IL-2 and IL-4) and their Co(II) complexes with concentrations of 5-35µg/ml were prepared. The overnight culture inoculum was prepared. 1 ml of compounds solutions of various concentrations were placed in a series of tubes and 0.4 ml of the inoculum was added to each tube. Further 4.5 ml of the sterile water was added to each of the test tubes. These test tubes were incubated for 22 hrs and observed for the presence of turbidity. The absorbance of the suspension of the inoculum was observed with spectrophotometer at 555 nm. The smallest concentration of antimicrobial (test materials) that produced a clear solution, i.e. no visible growth[xxx], was the final result of the test.

Docking study

Molecular docking is an important tool for studying the interactions of tiny molecules and macromolecules. Molecular docking evaluates the intermolecular interactions that occur between a ligand and a protein. In this paper, the docking studies of the designed Schiff bases and their Co(II) complexes have been carried out to predict the most possible type of interaction, the binding affinities and the orientations of the docked ligands at the active site of the target proteins. The starting geometry of the Schiff bases and their complexes were constructed using chem3D Ultra software (version 8.0, Cambridge soft Com., USA). The optimized geometry of Schiff bases and metal derivatives with the lowest energy was used for molecular dockings. The crystal structure of COVID-19 main protease complex with the inhibitor N3 (6LU7) was downloaded from the Protein Data Bank http://www.rcsb.org/structure/6LU7. AutoDockVina (Trott & Olson, 2010) was used to predict binding sites between the Schiff bases and their Co(II) metal complexes with 6LU7. The protein must be prepped for efficient insertion prior to the computation. As a result, all water molecules and ligands were eliminated from the active areas of the proteins. Partial atomic charges of the protease enzymes and Schiff base derivative molecules were calculated using Kollman methods.[xxxi] Active regions were identified as L287, D289, Q110, T292, G143, T111, F294 and S121. The grid box dimensions were calculated to be 100 * 95 * 95A° based on these active locations. The ‘x, y, and z' centres were also changed to 14.589, 34.523, and 66.124, respectively, before the 6LU7 protein was stored in PDBQT format for calculations. The next phase in the experiment was to find rotatable angles for coupling structures and record them in PDBQT format. For observations and preparations, the Discovery Studio Visualizer (Biovia, 2017) was utilized. AutoDockVina was used to do all the docking calculations. AutoDockVina determined twenty different adherences for the ligands attached to the protein's receptor. The best binding energies i,e -5.9 kcal mol^{-1} for ligand IL-1 and -7.1 kcal mol^{-1} for metal complex $[Co(IL\text{-}1)_2\ (H_2O)_2]$ were found in the initial calculation. As a result of its affinity and capacity to stick to active regions of the protein, could be a promising candidate for therapeutic design to treat severe acute respiratory syndrome caused by the new corona virus SARS CoV-2.

Results and discussion

The resulting novel Schiff based Cobalt (II) complexes are colored respectively light gray and brown solids and highly soluble in DMSO, ethanol, isopropyl alcohol, methanol, DMF but only sparingly soluble in water and toluene. Their monomeric nature is confirmed by their molecular weights. The reactions of metal salt $Co(OAc)_2.4H_2O$ with the Schiff base ligands were carried out in 1:1 and 1:2 ratios and trough the substitution of acetate ion followed metal complexes are formed [equations (1), (2)].

$$Co(OAc)_2.4H_2O + IL_{1\text{-}4} + NaOH \xrightarrow[\text{Ethanol}]{1:1} \left[Co(IL_{1\text{-}4})(OAc)(H_2O)_3\right] + NaOAc + 2H_2O \quad \text{------ (1)}$$

$$Co(OAc)_2.4H_2O + 2IL_{1\text{-}4} + 2NaOH \xrightarrow[\text{Ethanol}]{1:2} \left[Co(IL_{1\text{-}4})_2(H_2O)_2\right] + 2NaOAc + 4H_2O \quad \text{------ (2)}$$

The physical properties and analytical data of the ligands and their metal complexes, prepared by conventional thermal method as well as green chemical approach are illustrated in **Table-2 and Table-3(See Supporting Information)**.

Electronic spectra

The electronic spectra of all novel Schiff bases and their cobalt (II) complexes were recorded in the range of 190-1100 nm in DMSO **(Table-4)(See Supporting Information).**In the electronic spectra of Schiff base ligands display same behavior in 190-500 nm and shows two distinct bands in ranges 36364-38023 cm^{-1} (275-263 nm) and 29240-31646 cm^{-1}(342-316 nm) corresponds to spin-allowed transitions: π to π^* and n to π^*. On the other hand Co(II)complexes are expected three transition bands and are also observed experimentally. A consistent treatment for the bands is to assign the band near 9550-11654 cm^{-1} (1047-858 nm) as the $4T_{1g}$ (F) → $4T_{2g}$ (F) (ν_1) transition; the band at 16800-18790 cm^{-1}(595-532 nm) as the $^4T_{1g}$ (F) → $^4A_{2g}$ (F)(ν_2) transition and that at 20595-23100 cm^{-1}(486-433 nm) as the $^4T_{1g}$ (F) → $^4T_{1g}$ (P)(ν_3) transition. These three transitions suggest that an octahedral geometry is arisen around the Co^{+2} ion.[xxxii-xxxvii] The relative strength of the ligand and geometry of the complexes can be illustrated by calculating ligand field parameters like ligand field splitting energy (10 Dq), interelecyronic repulsion parameter (Racah parameter B), covalent factor (nephelauxetic ratio β) and band energy. These values have been calculated using standard equations.[xxxviii] The ligand field parameters show that Co(II) complexes possess an octahedral geometry with strong covalence **(Table-4). (See Supporting Information)).**

IR spectra

The FT-IR spectral data containing significant characteristic band regions of the novel ligands and its transition metal complexes are listed **in Table-5(See Supporting Information)**. The IR spectra of the heterocyclic ligands confirm a sharp band at 1567-1525 cm^{-1} region due to the appearance of an azomethine ν(C=N) but this band region is shifted to a lower frequency in all metal complexes spectral data, which endows that most likely azomethine nitrogen coordinates with the metal atom. Bands occurring in the 3294-3221 cm^{-1} region are due to ν(NH) vibrations in the spectra of free ligands but disappear in the spectra of complexes, which indicates deprotonation of the functional groups during the complexation process. In the spectra of ligands, medium intensity bands due to ν(C=S)/ν(C=O) vibrations arise in the ranges 1120-1098/1694-1684 cm^{-1} and are moved to a lower frequency in the spectra of complexes.[xxxix-xl] This is substantiated by the development of newer bands in the spectra of cobalt (II) complexes due to the ν(C-O) and ν(C-S) modes at lower frequencies. In the spectra of cobalt (II) complexes a band is observed in the range 880-865 cm^{-1} which may be attributed to the coordinated water molecule. Further, a broad band around 3472-3317 cm^{-1} may be due to ν(O-H) of water molecule. Bands in the region of 1497-1408 cm^{-1} and 1201-1148 cm^{-1}due to ν(Co-OAc) verify the unidentate coordination of

the OAc- anion and the occurrence of ν(Co-N), ν(Co-S) and ν(Co-O) vibrations are about 498-478 cm^{-1}, 450-431 cm^{-1}, and 452-429 cm^{-1}.[XIII] The other absorption bands for aromatic ν(C=C), ν(C–H), and aliphatic ν(C–H) appeared in their correct places. Thus, the FT-IR result concludes that the novel Schiff-base ligands in cobalt (II) complexes are binding through the azomethine nitrogen and oxygen/sulfur atom of amide/thioamide, respectively.

NMR spectra (^{1}H and ^{13}C)

The proposed structures of the ligands get further support by the ^{1}H-NMR and ^{13}C-NMR spectra of the ligands. The ^{1}H-NMR and ^{13}C-NMR spectra of the ligands were recorded in DMSO-d_6 w.r.t TMS (Trimethyl Silane) as reference at room temperature **(Table-6**). **(See Supporting Information)**

The ^{1}H-NMR spectrum of ligands semicarbazide and thiosemicarbazide (IL-1 and IL-2) exhibited a sharp singlet at same range 2.17ppm due to the (-CH_3) protons adjacent to thiophene ring, 7.12-7.13 ppm and 7.20-7.25 ppm due to aromatic protons (thiophene ring), 7.96 ppm and 7.51 ppm due to azomethine (-CH=N) proton, 10.18 ppm and 11.40 ppm for amide (-NHCO)/ (-NHCS) proton and for amine (-NH2) protons at 6.23 ppm and 8.17 ppm respectively. On the other hand a different pattern of NMR signals is observed for ligands IL-3 and IL-4. A sharp singlet at 2.20 ppm and 2.19 ppm due to the (-CH_3) protons adjacent to thiophene ring, 7.12-7.14 ppm and 7.22-7.24 ppm due to aromatic protons (thiophene ring), 8.28 ppm and 7.97 ppm due to azomethine (-CH=N) proton, 10.47 ppm and 10.20 ppm for amide (-NHCO)/ (-NHCS) proton and for amine (-NH2) proton at 7.18 ppm and 6.25 ppm were observed respectively. Due to the presence of methylene (-CH2-) and methyl (-CH_3) groups adjacent to amide (-NHCO)/ (-NHCS) a multiplates at 3.42-3.45 ppm and 4.12-4.16 ppm, a triplet at 1.03-1.07 ppm and 1.23-1.27 ppm were observed. Addition of D_2O results in diminishing the signals due to the –NH- and –NH_2 group. The ^{13}C NMR spectral data of the Schiff base ligands confirm the ^{1}H NMR spectral results. The ^{13}C NMR spectra of IL-1 to IL-4 shows that the azomethine carbon signal appears at the range 122.57-124.59ppm, C=O/C=S carbon signal appears at the range 151.64-177.48 ppm, methyl (-CH_3 adjacent to thiophene moiety) carbon appears at 15.23-17.84 ppm and all the four aromatic carbons appear at the range 130.76-133.45 ppm, 134.80-138.60 ppm, 137.51-139.23 ppm, 138.20-139.20 ppm. Due to the presence of additional methylene and methyl group in IL-3 and IL-4 show signals at 14.53 ppm and 14.89 ppm for methylene carbon and 60.62 ppm and 60.08 ppm for methyl carbon.

Mass spectra

The LC-MS data confirmed the mass of newly synthesized Schiff base ligands**.** The molecular ion peak obtained at *m/e* = 184 amu (M+1) for IL-1corresponds to calculated molecular formula $(C_7H_9N_3OS)^{+}$. As well as for IL-2, IL-3 and IL-4 the mass spectrum showed the molecular ion peak at 200.09 amu, 213.10 amu and 229.26 amu (M+1).

X-ray powder diffraction study

The possible lattice dynamics of the finely powdered products, [Co(IL-1)($OCOCH_3$)(H_2O)$_3$] has been deduced on the basis of X-ray powder diffraction studies[xli] at 2θ = 20-70° (Figure-1). The result shows that [Co(IL-1)($OCOCH_3$)(H_2O)$_3$]complex belongs to 'orthorhombic' crystal system [(a≠ b ≠ c) and α = β = γ = 90°] having unit cell parameters as a=9.55, b=17.89 c=22.13, maximum deviation of 2-Theta= 0.038-0.050^{o} , Alpha= 90^{o}, Beta= 90^{o}, Gama=90^{o}. We have tried to isolate single crystal of cobalt (II) complex suitable for X-ray diffraction study but could not succeed. However recently the single crystal structures of hexacoordinated cobalt (II) complexes have been reported in which the bidentate ligand adopts the most stereochemically favourable octahedral orientation.[xlii-xliv]

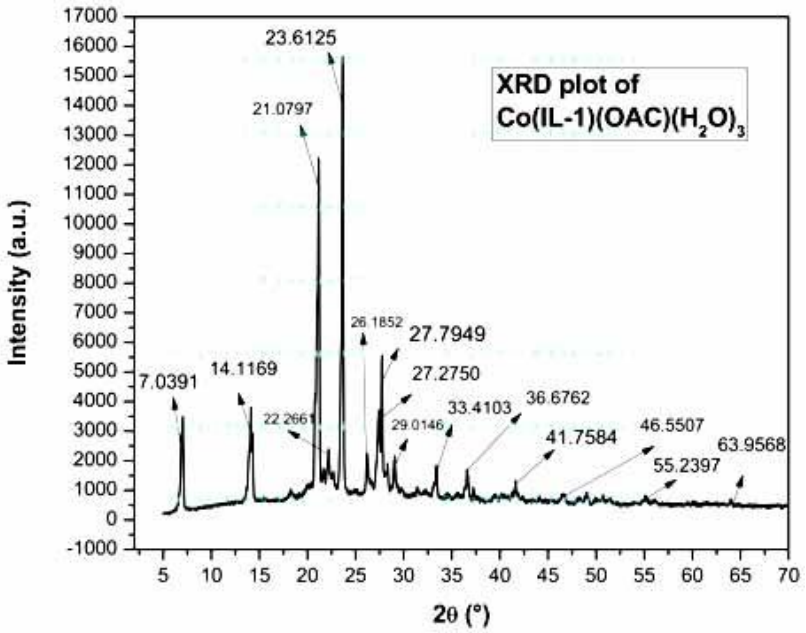

Figure-1:X-ray powder diffraction spectra of [Co(IL-1)(OCOCH$_3$)(H$_2$O)$_3$]

Molar conductivity

The conductivity bridge (G* = 1) was used to assess the molar conductance of all metal complexes at 25°C by preparing mmol solutions in 10^{-3} M DMF. The values obtained for metal complexes did not surpass $20\Omega^{-1}cm^2mol^{-1}$. This result indicates that metal complexes are non-electrolytic in nature.[xlv] The experimental values of the molar conductance research have been tabulated in **Table-7(See Supporting Information).**

Thermal analysis (TGA Study)

The thermal stability of these newly synthesized compounds was investigated using thermal gravimetric analysis as well as this technique was used to verify the status of water and solvent molecules inside or outside the coordination sphere of the complex compounds. Through simultaneous TGA analysis the weight loss of all novel Schiff bases and their metal complexes was measured from ambient temperature to 800°C by using alumina as a reference. The TGA results of these compounds matched well with the theoretical equations provided by spectrum analysis **(Table-8) (See Supporting Information).** The heating rates were well regulated at 10°C min^{-1} under nitrogen environment. At the final temperature, the breakdown pattern of metal complexes indicates the detachment of chelates, leaving respective metal oxides. The thermal stability and pattern of the decomposition process were found to be impacted by the attached anionic groups in metal salts, electronegativity, and atomic radius of metals.[xlvi-xlvii]

The anhydrous ligands (IL-1 to IL-4) show thermal stability up to 220°C and then degrade until it reaches 550°C, which is accompanied by a 68.25%, 63.03%, 59.21% and 55.04% mass loss, leaving more than 30.61-34.05% residue. This step corresponds to the loss of organic 4-methylthiophene-2-carbaldehyde moiety.

The TGA thermograms for 1: 1 Cobalt (II) complexes undergo three-step decomposition in the temperature range 50-800°C. The first stage of degradation occurred between 150 and 220°C in [Co(IL-1)(OCOCH$_3$)(H$_2$O)$_3$], [Co(IL-2)(OCOCH$_3$)(H$_2$O)$_3$], [Co(IL-3)(OCOCH$_3$)(H$_2$O)$_3$] and [Co(IL-4)(OCOCH$_3$)(H$_2$O)$_3$] complexes, which are accompanied by weight loss of 15.17%, 14.52%, 13.99% and 13.47% (Calcd. 15.27%, 14.61%, 14.11% and 13.54%), corresponding to the removal of three coordinated water molecules

respectively. The second decomposition step occurred by weight loss of 16.57%, 15.86%, 15.29% and 14.71% (Calcd. 16.68%, 15.96%, 15.41% and 14.80%) respectively between 221 and 380°C, which are associated with due to the loss of acetate group. In the last step, a mass loss of 51.37%, 53.46%, 54.90% and 56.82% (Calcd. 51.71%, 53.79%, 55.36% and 57.15%) consistent with the loss of organic ligand moiety (temperature range 381–800 ˚C) leaving cobalt oxides 5.11%-7.03% as residue.

In TGA curve of 1:2 cobalt (II) complexes does not show any weight loss up to 150°C. This indicates no lattice water molecules are present outside the sphere. The TGA thermograms for 1:2 Cobalt (II) complexes undergo two-step decomposition in the temperature range 50-800°C. The first stage of degradation occurred between 150 and 220°C in $[Co(IL\text{-}1)_2(H_2O)_2]$, $[Co(IL\text{-}2)_2(H_2O)_2]$, $[Co(IL\text{-}3)_2(H_2O)_2]$, and $[Co(IL\text{-}4)_2(H_2O)_2]$, complexes, which are accompanied by weight loss of 7.81%, 7.28%, 6.85% and 6.44%(Calcd. 7.84%, 7.33%, 6.96% and 6.56%) corresponding to the removal of two coordinated water molecules respectively. No weight losses are observed between temperature 221 and 380°C which confirm the absence of coordinated acetate groups inside complex. In the last step, a mass loss of 79.33%, 80.69%, 82.15% and 82.97% (Calcd. 79.69%, 80.98%, 81.96% and 82.98%) consistent with the loss of organic ligand moiety (temperature range 381–800 ˚C) leaving cobalt oxides 6.03% - 8.22% as residue.

The general scheme of stepwise decomposition of 1:1 and 1:2 metal complexes is shown below

$$\left[Co(IL_{1\text{-}4})(OCOCH_3)(H_2O)_3\right] \xrightarrow{150\text{-}220^\circ C} Co(IL_{1\text{-}4})(OCOCH_3)\Big] + 3\,H_2O$$

$$\left[Co(IL_{1\text{-}4})(OCOCH_3)\right] \xrightarrow{221\text{-}380^\circ C} \left[Co(IL_{1\text{-}4})\right] + CH_3COOH$$

$$\left[Co(IL_{1\text{-}4})\right] \xrightarrow{381\text{-}800^\circ C} IL_{1\text{-}4} + \text{Metal oxide (CoO)}$$

$$\left[Co(IL_{1\text{-}4})_2(H_2O)_2 \xrightarrow{150\text{-}220^\circ C} \left[Co(IL_{1\text{-}4})_2\right] + 2\,H_2O\right.$$

$$\left[Co(IL_{1\text{-}4})_2\right] \xrightarrow{381\text{-}800^\circ C} \left[2\,(IL_{1\text{-}4})\right] + \text{Metal oxide (CoO)}$$

It was concluded that the non-volatile nature of metal complexes was determined by the residues remaining near 800°C. Decompositions were occurred all almost the same rates in all of the complexes. The absence of lattice water molecules outside the coordination sphere is revealed by the stability of complexes up to 150°C.

On the basis of above studies octahedral environment around the metal atoms has been proposed and the expected structures are as shown in **Figure-2 and Figure-3.**

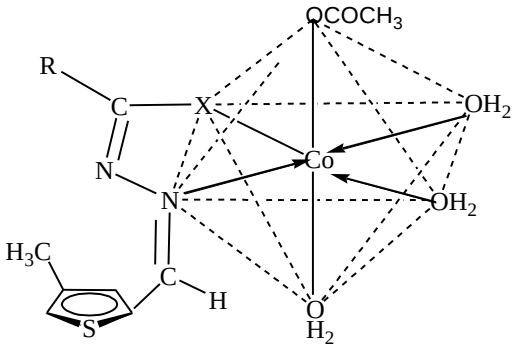

Where, R= -NH_2, -OCH_2CH_3
X= O/S

Figure-2: Suggested structures of cobalt (II) 1:1 metal complexes

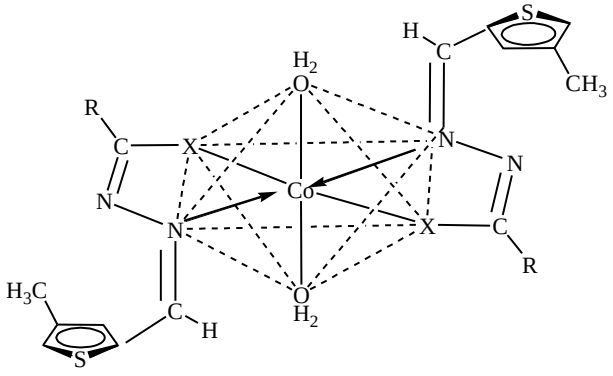

Where, R= -NH_2, -OCH_2CH_3
X= O/S

Figure-3: Suggested structures of cobalt (II) 1:2 metal complexes

Docking study

Molecular docking score, hydrogen bonds formation and the protein ligands interactions formed with the target protease (6LU7) of COVID-19 are summarized in **Table-9 (See Supporting Information)**. Because the protease enzyme is required for virus multiplication, blocking it is the primary goal of antiviral medication development. The ligand-enzyme interactions, as well as potential hydrogen bonds and electrostatic interactions, are also discussed. Any species with a higher negative binding energy value has a better docking capacity for target protein, and the docking of ligand and target protein was chosen based on the related binding energy value. The calculated binding energy values of the ligands (IL-1 to IL-4) with target protein were found to be -5.9 kcal/mol (IL-1), -4.8 kcal/mol (IL-2), -5.5 kcal/mol (IL-3) and -4.6 kcal/mol (IL-4) respectively and the calculated binding energy values of the novel cobalt (II) metal complexes (1:1 and 2:1 complexes) of the aforesaid species were -6.7 kcal/mol and -7.1 kcal/mol for [Co(IL-1)($OCOCH_3$)(H_2O)$_3$] and [Co(IL-1)$_2$(H_2O)$_2$], -5.8 kcal/mol and -6.2 kcal/mol for [Co(IL-2)($OCOCH_3$)(H_2O)$_3$] and [Co(IL-2)$_2$(H_2O)$_2$], -6.6 kcal/mol and -6.9 kcal/mol for [Co(IL-3)($OCOCH_3$)(H_2O)$_3$] and [Co(IL-3)$_2$(H_2O)$_2$] and -5.8 kcal/mol and -6.1 kcal/mol for [Co(IL-4)($OCOCH_3$)(H_2O)$_3$] and [Co(IL-4)$_2$(H_2O)$_2$]respectively **(Figure 4)**. According to docking results semicarbazide ligand (IL-1) and all newly synthesized cobalt (II) metal complexes show greater binding affinity than standard Favipiravir drug.

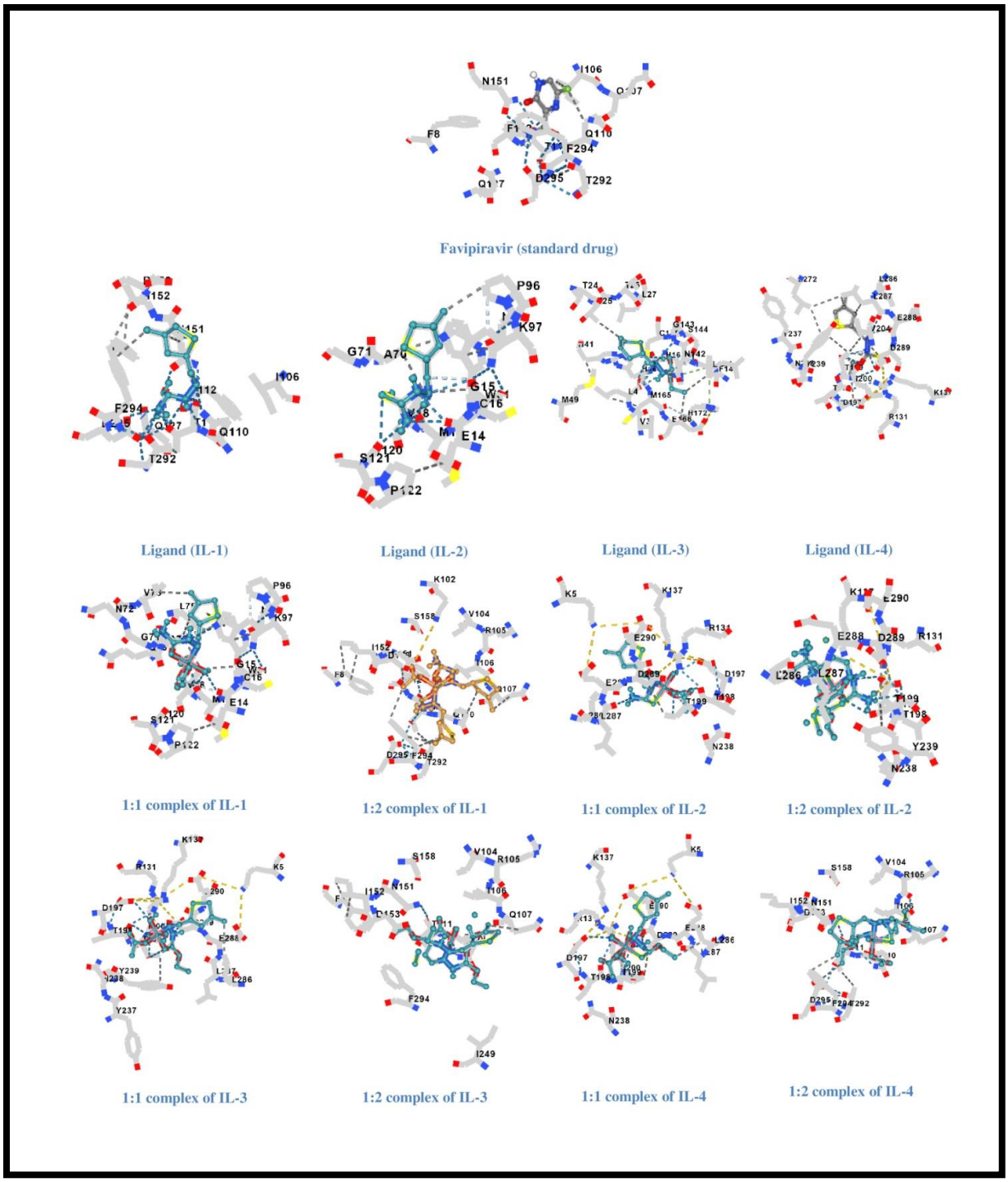

Figure-4: Docking between Favipiravir drug, ligands and their cobalt (II) complexes with COVID-19 main protease (6LU7) active site

Antimicrobial study

The antimicrobial activity of the heterocyclic Schiff base ligands and their cobalt (II) complexes was tested against two bacteria, *Bacillus subtilis* (Gram-positive) and *Escherichia coli* (Gram-negative), as well as two fungi, *Candida albicans* and *Aspergillus niger*, as shown in **Table-10 (See Supporting Information)**. When compared to parent ligands, metal chelates

had a higher activity, according to this study. On the basis of Overtone's theory and chelation theory**,** such increased activity of metal chelates can be explained. According to Overtone's concept of cell permeability, the lipid membrane that surrounds the cell priorities the passage of only lipid soluble molecules, making liposolubility a crucial aspect that regulates antimicrobial activity. The polarity of the metal ion is lowered to a higher extent during chelation due to ligand orbital overlap and partial sharing of the metal ion's positive charge with donor groups. It also improves the lipophilicity of complex by increasing the delocalization of p-electron across the entire ring. This increased lipophilicity allows the complexes to penetrate lipid membranes and inhibit metal binding sites on the microorganism's enzymes.[xlviii-l] The Minimal Inhibitory Concentration (MIC) values of newly synthesized compounds were also tested and results are illustrated in **Table-11 (See Supporting Information).** From the data, MIC values of metal complexes were showed lower than that of the parent Schiff base ligands. The antibacterial activities of metal complexes, $[Co(IL\text{-}2)(OCOCH_3)(H_2O)_3]$, $[Co(IL\text{-}2)_2\ (H_2O)_2]$, $[Co(IL\text{-}4)(OCOCH_3)(H_2O)_3]$ and $[Co(IL\text{-}4)_2\ (H_2O)_2]$ against *E. coli* (Gram-positive) were more effective with MIC value in the range of 14 to 20 µg/ml. In comparison these metal complexes were less effective against *Bacillus subtilis.*

Conclusion

The ligands and their cobalt (II) complexes synthesized through thermal as well as microwave methods were used for analyzing their physicochemical properties and antimicrobial activity. Microwave (MW) irradiation is an efficient technique and environmentally benign method to accomplish various inorganic/organic syntheses to afford products in higher yields in shorter reaction times. Monobasic bidentate Schiff bases (IL-1 to IL-4) and their cobalt (II) complexes in molar ratio (1:1) and (1:2) having the general formula $[Co(IL_{1\text{-}4})(OCOCH_3)(H_2O)_3]$ and $[Co(IL_{1\text{-}4})_2(H_2O)_2]$ were synthesized and characterized by various physicochemical techniques like FT-IR, NMR, mass, UV-Vis, TG analysis, elemental analysis, powder XRD. The above-mentioned techniques concluded bidentate nature (NO/NS) of Schiff base ligands which chelated via azomethine nitrogen and deprotonated carbonyl oxygen/sulfur in the enolised form with octahedral geometry around theCo^{2+} ion in entire complexes. Schiff base hydrazones and their Co(II) metal complexes were evaluated for their *in vitro* antimicrobial activity which revealed that complexes were more noxious than their respective Schiff base ligands against tested microbial strains under the same conditions. Further, cobalt (II) complexes of thiosemicarbazone were found to be the most potent among all the synthesized compounds. Additionally, the compounds also exhibited excellent molecular docking properties against the main protease (6LU7) of SARS-CoV-2. The docking results attributed various types of protein- ligand interactions and it is also seen that the Co(II) transition metal complexes show most significant interactions compared with well known drug 'Favipiravir' which is used worldwide for COVID-19 treatment.

Conflicts of interest:

There are no conflicts to declare.

Acknowledgements:

The authors are thankful to Bhupal Noble's University for providing laboratory facilities and financial support, University of Rajasthan for providing support in biological studies and SAIF, Panjab University for recording PXRD data.

References:

i. R. Yu, L. Chen, R. Lan, R. Shen and P. Li, *Int. J. Antimicrob. Agents.*, 2020, **56(2)**, 106012-106024. (https://doi.org/10.1016/j.ijantimicag.2020.106012)

ii. J. Wu, X. Yuan, B. Wang, R. Gu, W. Li, X. Xiang, L. Tang and H. Sun, *Frontiers. In. Microbiology.*, 2020, **11**, 1576-1603. (https://doi:10.3389/fmicb.2020.01576)

iii. A. K. Rana, S. N. Rahmatkar, A. Kumar and D. Singh, *Cytokine and Growth Factor Reviews*, 2020, **1**, 1-11. (https://doi:10.1016/j.cytogfr.2020.08.002)

iv. R. Mann, A. Perisetti, M. Gajendran, Z. Gandhi, C. Umapathy and H. Goyal, *Front. In. Med. (Lausanne).*, 2020, **7,** 1-12. (https://doi:10.3389/fmed.2020.581521)

v. S. Shrivastava, N. Fahmi and R. V. Singh, *Journal of Sulfur Chemistry*, 2010, **31(6)**, 515-524. (http://dx.doi.org/10.1080/17415993.2010.513438)

vi. R. Breslow, *Acc. Chem. Res.*, 1980, **13**, 170–174.

vii. S. Ahmad and M. Ali, *Appl. Catal. A: Gen.*, 2007, **331**, 149–153.

viii. J. Safari, S. H. Banitaba and S. D. Khalili, *Journal of Molecular Cataltsis A: Chemical*, 2011, **335**, 46-50.

ix. O. E. Sherif and N. S. Abdel-Kader, *Arabian Journal of Chemistry*, 2018, **11(5),** 700-713.

x. C. X. Zhang, C. Cui, M. Lu, L. Yu and y. x. Zhan, *Synth. React. Inorg. Met-Org. Nano-Met. Chem.*, 2009, **39**, 136-138.

xi. A. A. Jambol, M. S. Abdul Hamid, A. H. Mirza, M. S. Islam and M. R. Karim, *Int. J. of Org. Chem.*, 2017, **7**, 42-56.

xii. B. K. Rai and R. Kumari, *Orient. J. Chem.*, 2013, **29**, 1163-1167.

xiii. S. Chandra, Vandana and S. Kumar, *Spectrochimica Acta Part A: Molecular and Biomolecular Spectroscopy*, 2015, **135**, 356–363.

xiv. D. Mishra, S. Naskar, M. G. B. Drew and S. K. Chattopadhyay, *Inorg. Chim. Acta* , 2006**, 359**, 585–592.

xv. P. Sen, S. Z. Yıldız, Ö. Tamer, S. D. Kanmazalp and N. Dege, *Karadeniz. Chem. Sci. Tech.*, 2018, **03**, 01-05.

xvi. I. Kizilcikli, B. Ulkuseven, Y. Da sdemir and B. Akkurt, *Synth. React. Inorg. Met-Org. Chem.* 2004**, 34**, 653–665.

xvii. T. A. Yousef, G. M. Abu El-Reash, O. A. El-Gammal, and R. A. Bedier, *J. of Mol. Str.*, 2013, **1035**, 307-317.

xviii. R. A. Ahmadi and S. Amani, *Mol.*, 2012, **17**, 6434-6448.

xix. S. Shaygan, H. Pasdar, N. Foroughifar, M. Davallo and F. Motiee, *Appl. Sci.*, 2018, **8**, 85-97.

xx. A. A. A. Al-Riyahee, H. H. Hadadd and B. H. Jaaz, *Orient. J. Chem.*, 2018, **34(6)**, 2927-2941.

xxi. B. H. M. Mruthyunjiayaswamy, G. Y. Nagesh, M. Ramesh, B. Priyanka and B. Heena, *Der. Pharm. Chemica.*, 2015, **7(10),** 556-562.

xxii. C. Maria, A. Rodriguez, C. Estefania, A. Lopez-Silva, B. J. Sanmartin, C. A. Bacchi, C. C. Pelizzi and Z. Franca, *Inorg. Chimica. Acta.*, 2004, **357**, 2543-2552.

xxiii. K. Z. Laczkowski, K. Jachowicz, K. Misiura, A. Biernasiuk and A. Malam,

Heterocycl. Commun., 2015, **21(2),** 109-114.

xxiv. A.I. Vogel, A Textbook of Organic Quantitative Analysis, Fifth edition, 2004, 243.

xxv. J. Safari, S. H. Banitaba and S. D. Khalili, *J. of Mol. Cat. A: Chem.*, 2011, **335**, 46-50.

xxvi. M. B. Ferrari, S. Capacchi, G. Pelosi, P. Tarasconi, R. Alberitini, S. Pineli and P. Lunghi., *Inorg. Chim. Acta*. 1999, **286**, 134-141.

xxvii. C. H. Colins and P.M. Lyne, Microhiul Melfwds, p. 422, University Park Press, Baltimore (1970).

xxviii. K.S. Abou-Melha, *J.of Coordination Chem.*, 2008, **61(13),** 2053-2067.

xxix. S. A. Salmon, J. L. Watts and A. Cheryal, *J. Clin. Microbial*, 1995, **33(9)**, 2435-2444.

xxx. C. H. Collins, Antibiotics and antibacterial substances. In Microbiological Methods. Butterworths, London, 1964, 296.

xxxi. A. M. Gbaj, N. H. Meiqal, I. A. Sadawe, S. M. Beensaber, A .A. A. Alshoushan, M. S. Maamar and A. Hermann, *Lupine Online Journal of Medical Sciences*, 2020, **5(2),** 471-476.

xxxii. S. Chandra and A. Kumar, *Spectrochimica Acta Part A*, 2007, **66**, 1347–1351. (http://dx.doi.org/10.1016/j.saa.2006.04.047)

xxxiii. Y. M. Ahmed, M. M. Omar and G. G. Mohamed, *Journal of the Iranian Chemical Society*, 2021, 1-19. (https://doi.org/10.1007/s13738-021-02359-w)

xxxiv. W. H. Mahmoud, M. M. Omar, Y. M. Ahmed and G. G. Mohamed, *Appl. Organomet. Chem*., 2020, **34**, 1-20.

xxxv. M. M. Omar, G. G. Mohamed and A. A. Ibrahim, *Spectrochimica Acta Part A*, 2009, **73**, 358–369. (http://dx.doi.org/10.1016/j.saa.2009.02.043)

xxxvi. G. G. Mohamed, E. M. Zayed and A. M. M. Hindy, *Spectrochimica Acta Part A: Molecular and Biomolecular Spectroscopy*, 2015, **145**, 76-84. (http://dx.doi.org/10.1016/j.saa.2015.01.129)

xxxvii. S. Chandra and A. Kumar, *Spectrochimica Acta Part A*, 2005, **61**, 219-224. (http://dx.doi.org/10.1016/j.saa.2004.03.036)

xxxviii. A. B. P. Lever, *J. Chem. Educ.*, 1968, **45**, 711-712.

xxxix. S. Chandra and A. Kumar, *Spectrochim. Act. Part A*, 2007, **67**, 697-701.

xl. S. Chandra, Sangeetika, V.P. Tyagi and S. Raizada, *Synth. React. Inorg. Met. Org. Chem*., 2003, **33**, 147-164.

xli. A. A. Pawanoji and B. H. Mehta, *Asian Journal of Chemistry*, 2009, **21 (9),** 6869-6876.

xlii. E. N. Mainsah, S-J. E. Ntum, M. A. Conde, G. T. Chi, J. Raftery and P. T. Ndifon, *Crystal Structure Theory and Applications*, 2019, **8**, 45-56. (http://dx.doi.org/10.4236/csta.2019.84004)

xliii. J. X. Lin, M. L. Lin, Y. J. Su, M. S. Liu, H. P. Zeng and Y. P. Cai, *Transition Metal Chemistry*, 2007. **32**, 338-343. (http://dx.doi.org/10.1007/s11243-006-0173-3)

xliv. M. Kalitaa, P. Gogoia, P. Barmana and B. Sarma, *Journal of Coordination Chemistry*, 2014, **67(14),** 2445-2454. (http://dx.doi.org/10.1080/00958972.2014.946917)

xlv. W. J. Geary, *Coord. Chem. Rev*., 1971, **7**, 81-122. (http://dx.doi.org/10.1016/S0010-8545(00)80009-0)

xlvi. M. Yadav, S. Sharma and J. Devi, *J. Chem. Sci*.,2021, **133**, 21-43. (http://dx.doi.org/10.1007/s12039-020-01854-6)

xlvii. N. Kavith and P.V. A. Lakshmi, *J Saudi Chem Soc*., 2017, **21(1),** 457-466.

xlviii. S. M. El-Megharbel, A. M. Adam, A. S. Meghdad and M. S. Refat, *Russ. J.Gen. Chem*., 2015, **85,** 2366–2371. (http://dx.doi.org/10.1134/S1070363215100230)

xlix. B. H. Saghavaz, H. Pasdar and N. Foroughifar, *Biointerface Res. Appl. Chem*., 2016, **6**, 1842–1846.

l. R. Khadivi, H. Pasdar, N. Foroughifar, M. Davallo, *Biointerface. Res.Appl. Chem*., 2017, 7, 2238–2242.

Received on October 17, 2022.